Materials Characterization 120 (2016) 53–62

Contents lists available at ScienceDirect

Materials Characterization

journal homepage: www.elsevier.com/locate/matchar

Characterisation of weld zone reactions in dissimilar glass-to-aluminium pulsed picosecond laser welds

Octav P. Ciuca [a,*], Richard M. Carter [b], Philip B. Prangnell [a], Duncan P. Hand [b]

[a] School of Materials, University of Manchester, Manchester, M13 9PL, UK
[b] Institute of Photonics and Quantum Sciences, Heriot-Watt University, Edinburgh, EH14 4AS, UK

ARTICLE INFO

Article history:
Received 11 March 2016
Received in revised form 12 July 2016
Accepted 16 August 2016
Available online 16 August 2016

Keywords:
Ultrashort pulse laser
Microwelds
Interface reaction layer
Transitional alumina phases
Microstructure
Electron microscopy

ABSTRACT

Precision welded joints, produced between fused silica glass and aluminium by a newly-developed picosecond-pulse laser technique, have been analysed for the first time using a full range of electron microscopy methods. The welds were produced as lap joints by focusing a 1.2 μm diameter laser beam through the transparent glass top sheet, slightly below the surface of the metal bottom sheet. Despite the extremely short interaction time, extensive reaction was observed in the weld zone, which involved the formation of nanocrystalline silicon and at least two transitional alumina phases, γ- and δ-Al_2O_3. The weld formation process was found to be complex and involved: the formation of a constrained plasma cavity at the joint interface, non-linear absorption in the glass, and the creation of multiple secondary keyholes in the metal substrate by beam scattering. The joint area was found to expand outside of the main interaction volume, as the energy absorbed into the low conductivity and higher melting point silica glass sheet melted the aluminium surface across a wider contact area. The reasons for the appearance of nanocrystalline Si and transitional alumina reaction products within the welds are discussed.

1. Introduction

The ability to join glasses to metals, or to silicon, is an increasingly relevant technology for applications that include the manufacture of optical sensors, actuators, and the hermetic wafer-level encapsulation of electronic components in the production of MEMS and 'lab-on-a-chip' systems [1,2]. A range of processes are currently used for joining such very dissimilar materials, including; direct bonding [3,4], anodic bonding [1,5], glass frit joining [6], eutectic bonding or adhesive bonding [2, 7]. Unfortunately, these techniques are often poorly suited for glass-to-metal micro-joining due to intrinsic limitations, such as: the need for heat treatments, which may damage temperature-sensitive components [2,5,6], the development of residual stresses, resulting from the large difference in thermal expansion coefficients of the joined materials [2], and in-service issues that arise from polymer-based adhesives, like poor hermeticity [7], creep and outgassing.

In this context high pulse-rate laser microwelding is of growing interest, not only for avoiding the limitations imposed by the above techniques, but also because it offers the advantages of higher production rates and precise joint positioning. In addition, the extremely short thermal cycles induced by an ultrashort pulsed laser can in principle help prevent thermal damage and limit the formation of detrimental reaction products (e.g. intermetallic compounds, oxides, etc.) between dissimilar weld members at the joint interface [2].

With glass to glass welding it has been shown that successful microwelds can be produced using laser systems that deliver high-intensity, ultrashort (femto- or picosecond) laser pulses to the work piece [8–13]. This technique exploits the property of nonlinear optical absorption of the laser radiation in transparent materials, which allows the laser energy to be applied to a precise location within the workpiece volume in the vicinity of the beam focal point [9,13]. Thus, microweld lap joints can be achieved at the contact interface by focusing a pulsed laser beam through one of the glass sheets at the required depth. The resulting volume of molten glass generated, although small, is sufficient to fill the micron-scale gap between the glass sheets, which occurs by melt flow, driven by thermal expansion and the formation of a highly constrained plasma [8,12]. This micro-melt volume then solidifies to form the joint, and by translating the beam strong joints can be produced by controlling the net weld area (e.g. [8]).

Another major advantage of pulsed laser microwelding is that the heat-affected zone (HAZ) resulting from the microsecond-scale thermal cycles of a focused pulsed laser beam is much smaller than in the case of continuous fusion welding methods. The use of repeated short thermal cycles can also lead to significantly lower thermal stress levels between materials with very different thermal expansion coefficients and, thus, to welds less prone to cracking and premature failure [5,8,9,14].

In a more recent development the feasibility of using a picosecond pulsed laser to join silica glass to various metal substrates has been

* Corresponding author.
E-mail address: octav.ciuca@manchester.ac.uk (O.P. Ciuca).

http://dx.doi.org/10.1016/j.matchar.2016.08.013

demonstrated by the current authors [15]. In this work, the beam was transmitted through the glass sheet and focused into the metal surface, just below the joint interface. In all the weld samples produced by this method lap shear test pieces were found to fracture within the parent glass sheet, with the crack path travelling around the modified glass region, suggesting the welds had high interface bond strength. This is despite the fact that with certain glass-metal combinations there is a high thermodynamic driving force for chemical reaction to occur between the weld members. For example, when in contact with molten aluminium, under equilibrium conditions it is well known that SiO_2 will be reduced to form alpha-alumina and silicon [16–18]. Although currently little is known about the interface structure in metal-glass micro-laser welded joints, under the highly transient conditions found in picosecond pulsed laser welding, this reaction may not have time to occur and alternative metastable products may form (e.g. [19–21]).

Here, we aim to address this knowledge gap by reporting on the results of a detailed microstructural study performed on the interface region of glass-to-metal microwelds produced using a solid-state, 1030 nm, picosecond-pulsed laser with an average power of 2 W, between fused silica glass and aluminium. Of particular interest was to understand the mechanisms of weld formation and the extent of chemical reaction that takes place at the joint interface, as well as to determine the effects of the microwelding conditions specific to rapid laser pulsing on the resulting interface microstructure.

2. Materials and methods

A set of glass-metal micro welds was produced at Heriot-Watt University using a Trumpf TruMicro 5 × 50 laser with a pulse duration of 5.9 ps at a repetition rate of 400 kHz. To produce the welds, a 1 mm thick sheet of commercial purity aluminium (99.7%Al) was welded to a 1 mm thick sheet of fused silica glass with the spiral track pattern shown in Fig. 1(a). The fused silica glass grade chosen for this work was the ultra-high purity Spectrosil 2000, due to its excellent optical transmission for the laser wavelength used in the present experiments (1030 nm). The aluminium sheet was first polished to a mirror finish

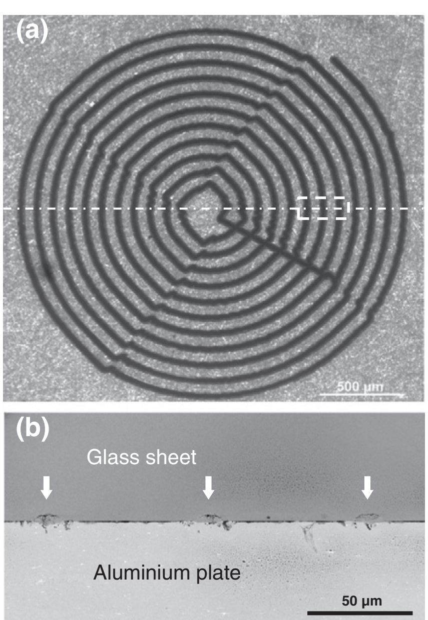

Fig. 1. Overview of the 2.5 mm diameter spiral-shaped weld areas produced by stage translation, with a pitch of 100 μm, and a travel speed of 1 mm·s^{-1}; (a) optical micrograph of the weld, viewed through the glass sheet; (b) low magnification SEM backscattered electron image of a typical cross-section through three neighbouring weld tracks, from the region indicated by the white rectangle in (a); the white arrows indicate the weld beads.

and then clamped against the glass using a pneumatically-actuated, four-point loading-jig that brought the two surfaces into close contact. A small area of optical contact was thus created above the jig piston. The jig assembly was mounted on a stage with motorized controls in the X and Y directions.

The laser beam was transmitted normal to the surface through the glass top sheet and the beam was focused slightly (~100 μm) below the interface of the two materials in the area of optical contact. The laser had an average power of 2 W and a focused spot size of 1.2 μm. The stage-mounted assembly was translated at a speed of 1 mm·s^{-1} under a stationary laser beam along a spiral path with a pitch of 0.1 mm to produce a continuous weld seam, resulting in a circular welded area with a final diameter of 2.5 mm (Fig. 1(a)). Small deviations from an ideal spiral, visible in the seam in Fig. 1(a), are the result of backlash of the x–y translation stage used. The microwelding procedure is described in full in [15].

To investigate the microstructure and phase distribution at the weld interface, representative weld areas were subsequently sectioned across their diameter to expose a cross-section through the weld seams (Fig. 1(b)). Metallographically prepared cross-sections were then investigated in an ultra-high resolution FEI Magellan 400 field-emission-gun scanning electron microscope (FEG-SEM) using backscattered electron (BSE) imaging at an accelerating voltage of 3 kV, and energy-dispersive X-ray spectroscopy (EDS) at 5 kV, in order to determine the morphology and phase composition of the weld regions. Small, site-specific samples were also extracted from the cross-sections of the welded interfaces and thinned to electron transparency using focused ion beam (FIB) milling, for analysis by transmission electron microscopy (TEM). The TEM samples were studied in an FEI Tecnai T20 microscope, in standard imaging and diffraction modes, and in STEM mode to obtain Z contrast by annular dark field (ADF) imaging and for elemental mapping by EDS.

3. Results

3.1. Weld zones

A surface overview of the welded area produced by translating the beam through the spiral pattern used in this study and a low magnification cross-section through three tracks is shown in Fig. 1. An SEM backscattered electron (BSE) image of a typical individual weld track is also provided in cross section in Fig. 2, along with a corresponding overlaid SEM-EDS elemental map, showing the coarse-scale distribution of the main elements (i.e. Si, O and Al) present in the two weld members. To aid interpretation, the main microstructurally distinct weld features described below have been labelled in Fig. 2(a). Further individual higher magnification elemental maps of the main central weld area are also provided in Fig. 3 along with a BSE image.

Overall, a complex chemically heterogeneous microstructure can be seen, containing cavities, porosity and microcracks, which is indicative of a highly energetic material-beam interaction and non-equilibrium reaction process. In Figs. 1 to 3 a significant amount of fine porosity, as well as coarse cavities, can be seen associated with each weld track. Caution is required in terms of interpreting the size and volume fraction of the cavities in the glass side of the weld, because the preparation of such a brittle sample by metallography is extremely difficult, without inadvertently removing some fragments from the porous weld regions. Nevertheless, in Fig. 2(a) it can be seen that at the laser beam position there is a main central weld zone, consisting of an approximately 20 μm wide semi-circular modified region in the glass top sheet. The images suggest that in the vicinity of the beam focus position there was a main plasma cavity in the glass top sheet that has subsequently partially collapsed, but there is also a secondary neighbouring cavity in the glass, in close proximity (to the right in Fig. 2(a)). Directly below the beam position and the main cavity there is clear evidence of a 5.5 μm deep keyhole being formed in the aluminium bottom sheet. In comparison, the keyhole in the aluminium surface under the secondary cavity in